JOURNAL OF GUIDANCE, CONTROL, AND DYNAMICS
Vol. 23, No. 1, January–February 2000

Simulation of Shot Impacts for the M1A1 Tank Gun

Ronald Gast* and Steven Morris†
Benet Laboratories, Watervliet, New York 12189
and
Mark Costello‡
Oregon State University, Corvallis, Oregon 97331

A validation of a coupled simulation package used for the accuracy assessment of large caliber weapons is reported. Test data from field firings of the M1A1 tank shooting M865 projectiles are compared with simulated results. The overall simulation predicts gun tube deformation during firing and projectile motion from the breech to the target. The gun tube is modeled using finite elements, and the projectile is modeled with finite elements while in the gun tube and as a rigid body while in free flight. By using this coupled analysis approach as compared to standard projection, a 42% improvement in the prediction of target impact locations for a select set of test conditions is realized.

Nomenclature

C_i	= projectile aerodynamic coefficients
D	= projectile characteristic length
D_C	= direction cosine matrix relating the gun and shot reference frames
F_t	= forcing function for gun, sabot, and projectile nodes
I	= mass moment of inertia matrix
L, M, N	= total external moments components on the projectile expressed in the body reference frame
M, C, K	= mass, damping, and stiffness matrix of the gun barrel, sabot, and projectile
m	= free-flight projectile mass
p, q, r	= components of the projectile angular velocity vector expressed in the body reference frame
p_e, q_e, r_e	= components of the projectile angular velocity vector expressed in the shot reference frame
$\boldsymbol{u}, \dot{\boldsymbol{u}}, \ddot{\boldsymbol{u}}$	= displacement, velocity, and acceleration vector for gun, sabot, and projectile nodes
u, v, w	= translation velocity components of the projectile center of mass resolved in the body reference frame
X, Y, Z	= total external force components on the projectile expressed in the body reference frame
x, y, z	= position vector components of the projectile center of mass expressed in the inertial reference frame
x_e, y_e, z_e	= position vector components of the center of the projectile base expressed in the gun reference frame
α	= longitudinal aerodynamic angle of attack
β	= lateral aerodynamic angle of attack
Δ	= stationline distance from the projectile base to mass center
ϕ, θ, ψ	= projectile Euler roll, pitch, and yaw angles

Introduction

NEVER has the need for simulation in the design of complex systems been more acute. Today's financial environment requires innovative thinking in the business of product development, especially for big ticket ordnance items. Future design efforts will rely on computational product development tools such as virtual performance simulation (VPS). Costs are greatly reduced because components reside in virtual space, allowing for rapid electronic design changes and performance ratings by simulation rather than physical testing. At the heart of VPS reside various analysis modules. Ultimately, these tools must be validated to achieve a level of comfort in their use. There are various ways to validate a simulation. First, one may use dedicated and controlled tests void of extraneous noise to establish relational characteristics among a few test variables. The results may then be compared to simulations produced using the same range of independent design variables, and validation is achieved when the test and model output responses produce nearly the same results. The second method involves the use of field-generated data to compare with results of simulations. The field data may contain extraneous noise as well as unknown system traits that affect response. The best one may expect to achieve from this type of validation is trends in the responses relative to variations in the system parameters. This is a type of differential analysis and is more prevalent for the validation of fully operational systems such as fielded ordnance weapons. As the controllable design variables are changed, results yield response trends. Because the test data used here have been generated during field firings of the weapon, the second method of validation applies.

It is well known from previous experiments that shot impact patterns are a strong function of the particular tube used for firing.[1–4] Every manufactured gun tube has its own signature regarding its dynamic response during firing and, more importantly, projectile exit conditions from the tube. This not withstanding, fire control systems apply a so-called fleet zero global correction factor to shot impact points for all tanks of a given model. This has led to the development of gun jump correction factors applicable to a specific tank and gun combination that are applied to the fleet zero corrections just mentioned. Obviously, experimental generation of gun jump correction factors is an expensive proposition requiring multiple test firings of every tank, gun tube, and projectile combination. The potential to supplement and replace portions of this test procedure with VPS is particularly attractive from a time and money point of view. By validating fully coupled gun tube and projectile dynamics from the breech to target impact for an operational system, the current effort moves closer toward this goal.

Dynamic Indexing of Gun Tubes

The M256 cannon has characteristics that cause transverse gun vibrations during firing. One of these is due to the offset breech that is below the bore centerline. As the gun recoils, this offset mass produces an inertia couple that transmits a vibration wave along the tube's axis, overtaking the projectile and disturbing the muzzle before shot exit from the gun tube. Also, as the projectile travels along the bore, interactive loads develop between the tube and the projectile causing additional vibrations of both. On exit, the intended direction of the round has been compromised. The effect is mitigated, as Schmidt[1] suggests, by specifying a characteristic

Received 11 February 1999; revision received 1 June 1999; accepted for publication 1 June 1999.

*Special Projects Team Leader, Benet Laboratories, Watervliet Arsenal.
†Special Projects Mechanical Engineer, Benet Laboratories, Watervliet Arsenal.
‡Assistant Professor, Department of Mechanical Engineering.

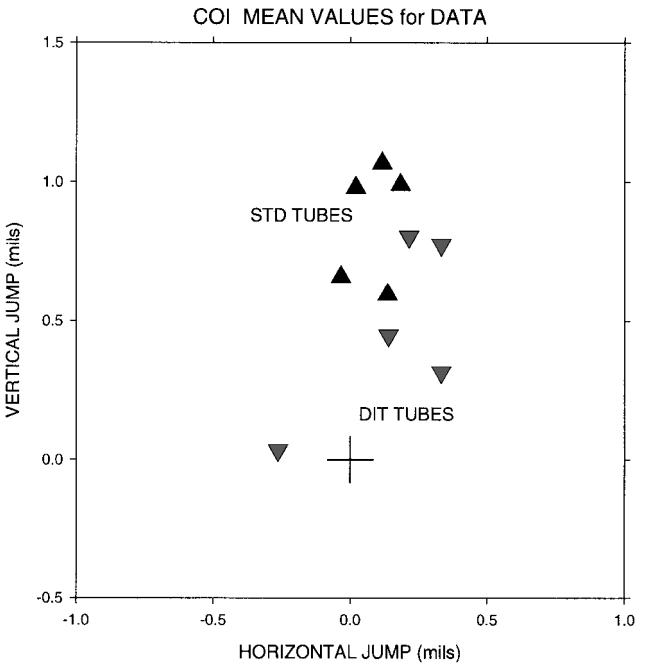

Fig. 1 COI results for 10 tubes in test.

bore profile that minimizes the global vibratory nature of projectile/tube/offset mass interaction. Based on dynamic analysis, a tube possessing an optimum profile provides a relatively straight path for the projectile to follow. This minimizes side loads and projectile cross-axis deflections rendering a benign entrance into free flight void of asymmetric kinematic excitations. The method of implementing this feature is called dynamic indexing of the tube (DIT). In contrast to DIT, the standard method of tube indexing (STD) is to orient the top vertical centerline of the gun such that the plane of greatest bending is vertical and the gun tube muzzle points up. This method tends to minimize curvature due to gravity droop when the cannon is mounted in its vehicle.

To verify the DIT methodology, extensive firing tests were performed and reported by Webb et al.[2] The subsequent experimental impact data are extracted from this work for five DIT- and five STD-type tubes. The cannons were mounted on M1A1 vehicles and accuracy tests were performed with several different 120-mm ammunition types. Each tube fired three rounds using each round type and condition temperature. The centers of impact (COI) and target impact dispersion (TID) were the primary data reported and represent the test data used in this study.

In Fig. 1, the average COI values for the 10 tubes are presented. In the chart the inverted triangular symbols refer to the DIT tubes whereas the upright triangular symbols refer to the STD tubes. With the exception of one flier for the DIT group, the remaining four responses seem to reside in close proximity in the plot, whereas the five from the STD group reside at a different location. Whereas the DIT gun tubes tend to bring the impact points in line with the aim point, dispersion and impact point characteristics remain the same.

Gun Tube and In-Bore Projectile Dynamic Model

The dynamic and kinematic states of the gun tube and projectile are simulated using the simulation analysis tool simulation of barrel dynamics (SIMBAD). SIMBAD is designed to predict the motion of the gun barrel and projectile during the firing phase and ultimately passes the exit conditions of the projectile to the flight prediction model to assess the flight path to the target.

The basic model for the analysis reported herein consists of a three-dimensional beam finite element structural representation for the gun barrel using an Euler–Bernoulli formulation for the partial differential equation of a dynamically loaded elastic beam. The barrel structure is attached to a rigid cradle through nonlinear elastic elements at two locations, one near the breech and one near the forward support. In addition, the barrel may have rigid bodies attached to its nodal points for the modeling of the breech, bore evacuator, and muzzle brake or muzzle reference system. These masses are treated as pure inertia elements with fully populated matrices and, as such, may be offset with respect to the node to which they are attached. Barrel droop due to gravity and centerline profile distributions due to manufacturing may be simulated as well.

The shot is represented as a two-piece flexible structure consisting of a projectile and sabot. Both are modeled using beam finite elements, much like the barrel. The shot interacts with the barrel through the bore rider portion of the sabot. Nonlinear stiffness is used for the force transfer at these locations. The projectile interacts with the sabot in the same manner; however, stiffness in the axial direction is included that allows for relative motion between the two components.

As with all standard finite element models, the dynamic equation for barrel, sabot, and projectile is cast in a matrix form as

$$[M]\{\ddot{u}\} + [C]\{\dot{u}\} + [K]\{u\} = \{F_t\} \tag{1}$$

Equation (1) represents a set of simultaneous second-order differential equations whose matrix coefficients M, C, and K are formulated using well-known finite element techniques. The forcing function F_t consists of contributions from ballistic pressure, reaction forces between the gun and the projectile, as well as reactions from the supporting structure. A time–marching procedure based on a modified Runge–Kutta technique is used to integrate the equations.

For the study conducted herein, the tube employs a 40-element Euler beam model and 41 nodes. The centerline profiles for the 10 gun tubes used in this study have been determined using statistical methods to be described later. The cradle, which is "ground" for this study, is connected to the tube through the use of nonlinear elastic support elements. The projectile and sabot are both modeled using seven finite elements with an additional mass for the penetrator's tail fin. The sabot and gun tube are coupled at two points through nonlinear stiffness elements using data from a static test.

A simplified sabot decompression scheme mechanically perturbs the projectile's exit kinematics. It is a linear decompression model that augments the initial in-flight conditions of the projectile. Because the SIMBAD model employs a two-piece shot (i.e., projectile and sabot) that is elastically linked at two points along its axes, a state of strain exists between the two during in-travel and at exit from the tube. The disengagement model assumes that this strain is relieved at exit, thus imparting forces and moments to both the sabot and the projectile. Employing momentum and energy conservation principles and using the inertial properties of the sabot and projectile result in additional transverse and rotational velocity being imparted to both on disengagement. The effect on the projectile is directly input into the exterior ballistics model that contributes to the free-flight trajectory to target. The aerodynamic interaction between the disengaging sabot and projectile is not considered in this model.

Free-Flight Projectile Dynamic Model

The mathematical model describing projectile motion admits six rigid-body degrees of freedom composed of three body inertial position coordinates as well as three Euler angle body attitudes. The equations presented hereafter use the ground surface as an inertial reference frame. The body frame is defined in the conventional manner[5] and the dynamic equations are written with respect to this coordinate system. The projectile translation and rotation kinematic and dynamic equations are given by (see Refs. 5 and 6)

$$\begin{Bmatrix} \dot{x} \\ \dot{y} \\ \dot{z} \end{Bmatrix} = \begin{bmatrix} c_\theta c_\psi & s_\phi s_\theta c_\psi - c_\phi s_\psi & c_\phi s_\theta c_\psi + s_\phi s_\psi \\ c_\theta s_\psi & s_\phi s_\theta s_\psi + c_\phi c_\psi & c_\phi s_\theta s_\psi - s_\phi c_\psi \\ -s_\theta & s_\phi c_\theta & c_\phi c_\theta \end{bmatrix} \begin{Bmatrix} u \\ v \\ w \end{Bmatrix} \tag{2}$$

$$\begin{Bmatrix} \dot{\phi} \\ \dot{\theta} \\ \dot{\psi} \end{Bmatrix} = \begin{bmatrix} 1 & s_\phi t_\theta & c_\phi t_\theta \\ 0 & c_\phi & -s_\phi \\ 0 & s_\phi / c_\theta & c_\phi / c_\theta \end{bmatrix} \begin{Bmatrix} p \\ q \\ r \end{Bmatrix} \tag{3}$$

$$\begin{Bmatrix} \dot{u} \\ \dot{v} \\ \dot{w} \end{Bmatrix} = \begin{Bmatrix} X/m \\ Y/m \\ Z/m \end{Bmatrix} - \begin{bmatrix} 0 & -r & q \\ r & 0 & -p \\ -q & p & 0 \end{bmatrix} \begin{Bmatrix} u \\ v \\ w \end{Bmatrix} \tag{4}$$

$$\begin{Bmatrix} \dot{p} \\ \dot{q} \\ \dot{r} \end{Bmatrix} = [I]^{-1} \left[\begin{Bmatrix} L \\ M \\ N \end{Bmatrix} - \begin{bmatrix} 0 & -r & q \\ r & 0 & -p \\ -q & p & 0 \end{bmatrix} [I] \begin{Bmatrix} p \\ q \\ r \end{Bmatrix} \right] \quad (5)$$

The total applied force is composed of weight W and body aerodynamic force A terms. The weight portion of the external loads is given by

$$\begin{Bmatrix} X_W \\ Y_W \\ Z_W \end{Bmatrix} = mg \begin{Bmatrix} -s_\theta \\ s_\phi c_\theta \\ c_\phi c_\theta \end{Bmatrix} \quad (6)$$

whereas the aerodynamic force contribution is given by

$$\begin{Bmatrix} X_A \\ Y_A \\ Z_A \end{Bmatrix} = -\tilde{q}_a \begin{Bmatrix} C_{X0} + C_{X2}(\alpha^2 + \beta^2) \\ C_{NA}\beta \\ C_{NA}\alpha \end{Bmatrix} \quad (7)$$

$$\alpha = \tan^{-1}(w/u), \qquad \beta = \tan^{-1}(v/u) \quad (8)$$

$$\tilde{q}_a = \tfrac{1}{8}\rho(u^2 + v^2 + w^2)\pi D^2 \quad (9)$$

The right-hand side of the rotation kinetic equations contains the externally applied moments. The external moment components contain contributions from steady SA and unsteady UA body aerodynamics. The steady body aerodynamic moment is computed by a cross product between the distance vector from the center of gravity to the center of pressure and the steady body aerodynamic force vector just given. Like the aerodynamic coefficients, the center of pressure location is dependent on local Mach and is computed by linear interpolation. The unsteady body aerodynamic moment provides a damping source for projectile angular motion and is given by

$$\begin{Bmatrix} L_{\mathrm{UA}} \\ M_{\mathrm{UA}} \\ N_{\mathrm{UA}} \end{Bmatrix} = \bar{q}_a D \begin{Bmatrix} C_{DD} + pDC_{LP}/2V \\ qDC_{MQ}/2V \\ rDC_{NR}/2V \end{Bmatrix} \quad (10)$$

Air density is computed using the center of gravity position of the projectile in concert with the standard atmosphere.[7] The free-flight projectile model described in this section has been validated against spark range data for a generic 25-mm fin-stabilized sabot launched projectile,[8] and agreement between the model and range data is good.

Model Matching Conditions

For proper coupling between the in-bore and free-flight projectile models, the kinematic state must be transferred from the in-bore dynamic model to the free-flight model. Because the in-bore and free-flight models use different coordinates, matching conditions are nontrivial. The in-bore dynamic model uses two frames, namely, a gun frame that is attached to the undeformed tube and is aligned with the tube axis and a shot frame that is attached to the projectile. The origin of the gun frame is at the breech and the origin of the shot frame is the center of the base plate of the projectile. The free-flight projectile model uses an inertial frame that is attached and aligned with the ground plane and a body frame that is attached to the projectile. The origin of the inertial frame is the breech and the origin of the body frame is the projectile mass center. At shot exit, the interior ballistics output includes the following items: gun elevation angle, direction cosine matrix relating the gun and shot frames, gun frame components of the position of the base of the projectile, gun frame components of the velocity of the projectile mass center, and shot frame components of the projectile angular velocity vector.

The transformation from the inertial to body frame using coordinates from the in-bore analysis is given as

$$T_{IB} = \begin{bmatrix} c_{\mathrm{QE}} & -s_{\mathrm{QE}} & 0 \\ 0 & 0 & 1 \\ -s_{\mathrm{QE}} & s_{\mathrm{QE}} & 0 \end{bmatrix} [D_C] \begin{bmatrix} 1 & 0 & 0 \\ 0 & 0 & -1 \\ 0 & 1 & 0 \end{bmatrix} \quad (11)$$

The gun quadrant elevation angle (QE) relates the gun and inertial frames. Using this definition, the initial state of the projectile for the free-flight analysis is obtained from the exit conditions of the in-bore analysis using

$$\begin{Bmatrix} x_0 \\ y_0 \\ z_0 \end{Bmatrix} = \begin{bmatrix} c_{\mathrm{QE}} & -s_{\mathrm{QE}} & 0 \\ 0 & 0 & 1 \\ -s_{\mathrm{QE}} & s_{\mathrm{QE}} & 0 \end{bmatrix} \left[\begin{Bmatrix} x_E \\ y_E \\ z_E \end{Bmatrix} + [D_C] \begin{Bmatrix} \Delta \\ 0 \\ 0 \end{Bmatrix} \right] \quad (12)$$

$$\begin{Bmatrix} u_0 \\ v_0 \\ w_0 \end{Bmatrix} = \begin{bmatrix} c_{\mathrm{QE}} & -s_{\mathrm{QE}} & 0 \\ 0 & 0 & 1 \\ -s_{\mathrm{QE}} & s_{\mathrm{QE}} & 0 \end{bmatrix} [D_C]^T \begin{Bmatrix} \dot{x}_E \\ \dot{y}_E \\ \dot{z}_E \end{Bmatrix} \quad (13)$$

$$\theta_0 = \sin^{-1}(-D_{C_{3,1}}) \quad (14)$$

$$\phi_0 = \sin^{-1}(D_{C_{3,2}} / \cos\theta_0) \quad (15)$$

$$\psi_0 = \sin^{-1}(D_{C_{2,1}} / \cos\theta_0) \quad (16)$$

$$\begin{Bmatrix} p_0 \\ q_0 \\ r_0 \end{Bmatrix} = \begin{bmatrix} 1 & 0 & 0 \\ 0 & 0 & -1 \\ 0 & 1 & 0 \end{bmatrix} \begin{Bmatrix} p_E \\ q_E \\ r_E \end{Bmatrix} \quad (17)$$

Also, the in-bore dynamic model includes structural deformation degrees of freedom, whereas the free-flight model is rigid. The mismatch in degrees of freedom is handled by fitting the deformed projectile shape with a line using regression. The rigid-body states are then extracted from the line properties.

Configuration Analysis

Generating simulation results obviously requires knowledge of many system parameters, and some of these parameters were not recorded during field tests. To deal with this problem, parametric methods of analysis are used. Nominal values for unknown parameters considered important are incremented within a range with simulations being conducted for every combination of parameters. Thus, a distribution of shot impact locations for a given gun tube is generated. Computed and test results are then compared on the basis of both mean value and standard deviation.

It is well known that the condition of the gun tube's centerline profile affects the in-bore vibration response of both the tube and round,[3] as well as the mean impact location and dispersion of the shots fired during an accuracy test.[2] Bore profile curvature is a particularly important parameter.[3,4] For the test data used here, bore profile measurements were taken using a mechanical procedure. The inspection interval along the tube was approximately 0.75 ft for a total of 23 measurement stations. Profile measurements were subject to an error of approximately 0.00118 in. The measured bore profile data are to be used to generate a representative smooth profile that possesses the necessary curvature information to calculate the interactive forces between the accelerating projectile and the gun tube. The means of achieving this is to generate a polynomial fit of the data using a least-squares technique. The chi-squared statistic[9] is used to optimize the polynomial order for the bore profile fit.

The M865 kinetic energy training round was used in the test data and a basic schematic is shown in Fig. 2. It employs three aluminum sabot pedals, an aluminum tail fin, and a low alloy steel projectile. Even though the sabot is flexible, the in-bore model requires explicit specifications for the force/penetration data at the contacting surfaces between sabot bore riders and tube inner diameter at both the front and rear contact points. Lyon[10] conducted stiffness tests for this round and has provided experimental data for both locations. The stiffness is nonlinear for both areas. Material resistance is small during initial sabot deflection and then gradually increases as deflection becomes greater. Also, due to the three separate sabot petals, the assembly stiffness is a function of the location around the azimuth. For example, if the projectile is oriented such that the load is applied to the circumferential center of a petal, its stiffness is different than if the load were applied at the joint between two

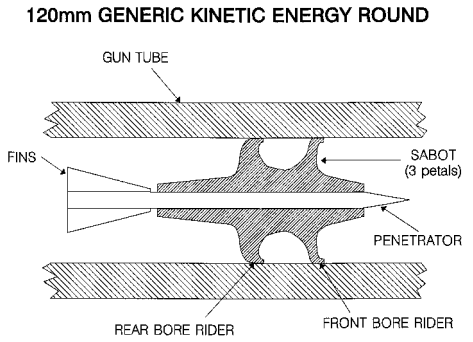

Fig. 2 Trainer round schematic for 120-mm M865.

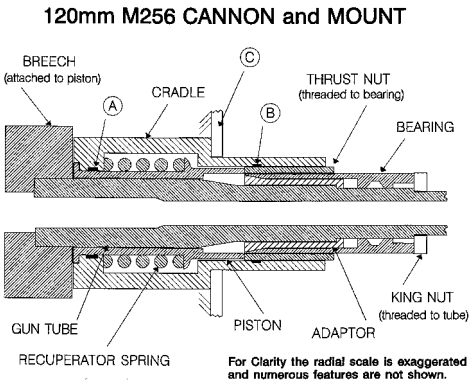

Fig. 3 M1A1 gun mount schematic.

petals. The stiffness range around the periphery has a 15% variation from the maximum stiffness value.

As with the projectile-to-tube interface, the tube-to-mount interface must be explicitly defined. The mounting specifications are characterized by nonlinear spring elements applied at the gun's mounting locations. A schematic of the major components involved in the mounting of the gun is shown in Fig. 3. Points A and B are seal locations within which the recoil fluid resides. These points are also considered the cannon's mounting points for vibration analysis. The spring located in this chamber compresses between the piston head and rear surface of the cradle during recoil. It provides the necessary energy to return the cannon to its in-battery position. All components except the cradle are subject to recoil motion and the major level of transverse vibration. The adapter, which has an internal profile closely matching the gun tube's outer profile, is held in place by the bearing, which drives the adapter inward thus engaging the tube's outer surface. The king nut, which is threaded to the outer surface of the tube, provides the clamping force to maintain the bearing/adapter assembled to the tube. The thrust nut is the link that marries together all of the recoiling components. It has an internal thread that engages a mating thread on the outer diameter of the bearing. When tightened, the load pulls the cannon and piston forward through the bearing, king nut, tube, and breech threads. The cradle is assumed to be grounded along the face at the shoulder located just forward of the fluid and spring chamber. This represents the forward end of the rotor and is considered grounded with respect to the vibrating cannon.

Through the examination of the relevant component drawings, the range of clearances between recoiling and stationary parts in the assembly are 0.005–0.010 in. at point A and 0.001–0.011 in. at point B. When the cannon is within the clearance, its transverse motion will be unopposed by any external loads except its own inertia. However, when the king nut is tightened to its preload specification, the clearance between recoiling and nonrecoiling components decreases considerably. Wilkerson has measured these clearance values and has determined that at most 0.002 in. is realizable at either location (S. Wilkerson, Army Research Laboratory, Aberdeen, Maryland and R. Gast, Benet Laboratories, Watervliet, New York, 1995, private communication).

Table 1 Uncertain parameter values

Parameter	Nominal value	Range of values
Peak ballistic pressure	53,400 psi	±2.5%
Mount clearance	0.001 in.	0–0.002 in.
Average stiffness of mount	5.0×10^6 lb/in.	±5%
Rear bore rider stiffness	513.0×10^3 lb/in.	±5%
Front bore rider stiffness	236.0×10^3 lb/in.	±5%

To determine structural resistance during contact, a twofold approach is employed. Because the cradle is assumed to be grounded along its midaxial location, both the breech and the muzzle end resemble short cantilever beams. Stiffness values using beam theory alone yield overly large value for stiffness. An alternative method using Hertzian contact stress applied in series with beam theory is employed. Unlike the beam model, whose stiffness is constant regardless of the level of deformation, the interface stiffness in the Hertzian model begins at zero and rapidly rises in a nonlinear fashion for increasing penetration of one material into the other. By employing these two models in series, a slightly nonlinear load-deflection distribution is determined.

The ballistic performance of a particular round is usually recorded during a test in the form of peak propellant gas pressure and muzzle velocity. Variations in these values from shot to shot are common. For this test, such data were not retained; therefore, a nominal distribution for gas pressure generated from a ballistic simulation is used in this study.

Whenever an accuracy test is performed, the aiming of the weapon is an issue. Super elevation is a term that addresses the amount of elevation loss that a projectile endures as it traverses downrange. It is the amount of additional rotational elevation that must be applied to the weapon, after the muzzle has been aimed at the cross hairs of the target, for the projectile to arrive at the proper impact location under the influence of gravity drop. This is a function of target range and, although tank weapons are used for direct fire applications, it still must be considered. In addition, because every gun tube has its own specific bore centerline profile that is additive to gravity droop, the amount of total elevation will be different from tube to tube. To determine the total elevation, the individual slopes, both horizontal and vertical, of the muzzle are used. These slopes are determined by calculating the average slope of the secants connecting the last three nodes of the gun tube. The nodal locations from the in-bore model of each gun tube in its gravity drooped state are used for these calculations. Correctly prescribing these values is important with respect to the free-flight model because projectile orientation with respect to gravity is a dominant load during free flight of the round. This parameter was set for each tube in the study and was not varied to induce any dispersion-causing effects.

By using the methods, assumptions, and data as indicated, the nominal values and ranges for the uncertain parameters were determined and are shown in Table 1.

Results of Analysis

In Figs. 4a–4c, the results for a select number of tubes in the test are presented as target impact plots of the actual and simulated firings. These results are contained on the rightmost portion of Fig. 4. In addition, the bore profile measurement data and the statistically generated polynomial fits are shown on the leftmost portion. The upper plot on the left contains data for the vertical centerline profile, whereas the plot directly below contains the same for the horizontal direction. Two shot impact assessment methods are shown in the plots. The points labeled SIMBAD JUMP at EXIT represent the simulated impact point as a linear extrapolation from the projectile's exit conditions. In the discussion to follow, this result is dubbed the SIMBAD analysis. The points labeled BOOM JUMP at TARGET represent the simulated impact points using the fully coupled in-bore and free-flight models described earlier. In the discussion to follow, this simulation is called the BOOM analysis. The impact scale is angular with a range of 2.0 mils. The center of each impact circle locates the mean value for each result, whereas the diameter represents the 1-sigma circular dispersion band. Presentation in this manner lends itself to a concise and multifaceted comparison

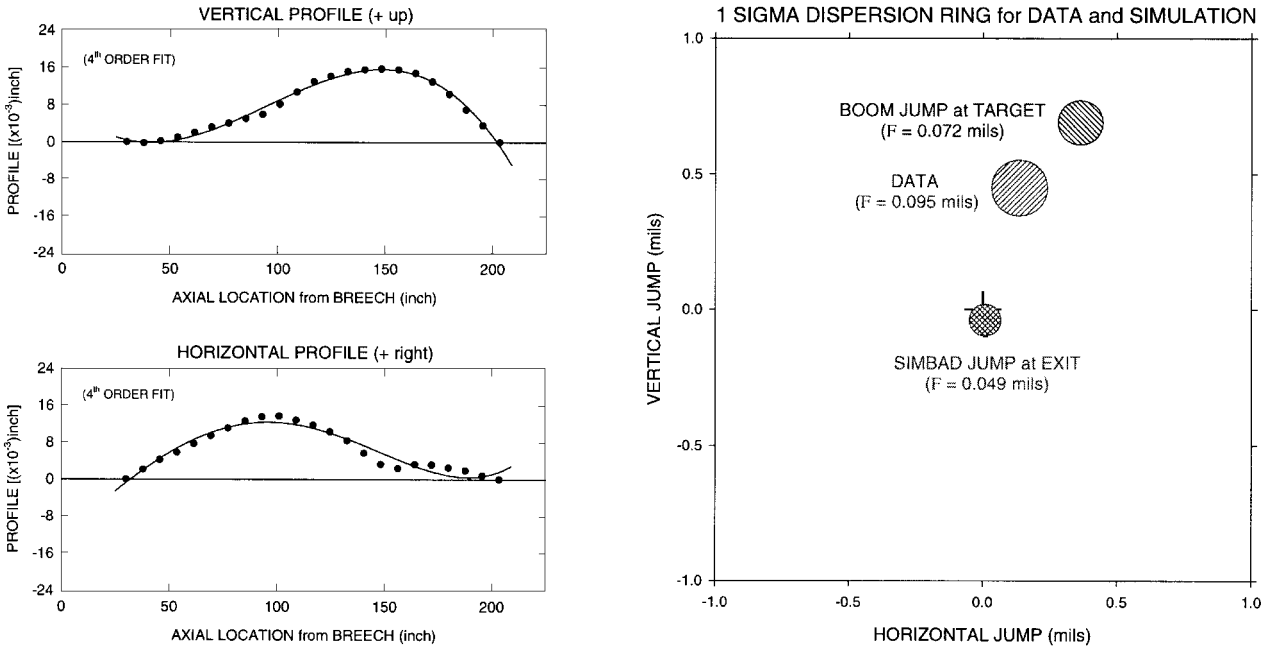

Fig. 4a Comparison of results for tube 4100.

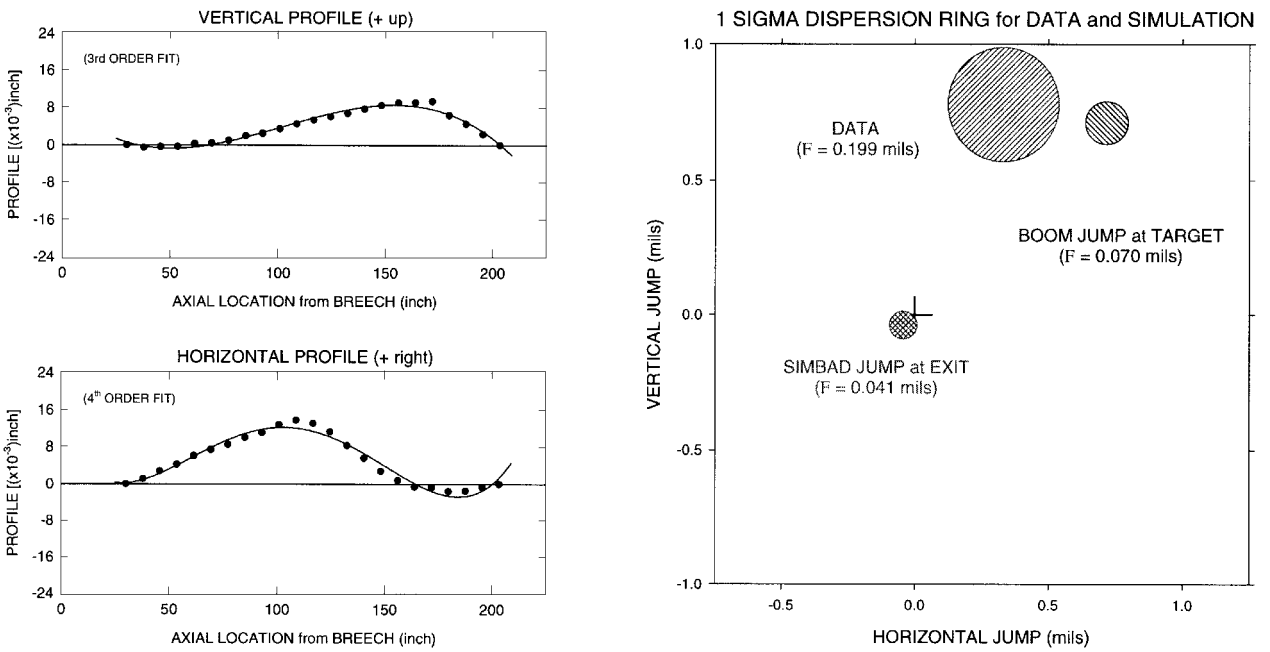

Fig. 4b Comparison of results for tube 4106.

between the data and the results. Because of space limitations, the results from only 3 of the 10 tubes in the analysis are shown and discussed at length. A summary of the mean value analysis for all 10 tubes will be reported at the end of this section.

Results for tube 4100 (DIT tube) are shown on Fig. 4a. Note the orientation of the centerline profile in the vertical direction. It is a large bow that points down at the muzzle. This tube was purposely indexed during manufacture to achieve this condition. The statistical analysis of the measurement data (closed circles) indicates that a fourth-order polynomial is the appropriate. In the horizontal plane a similar shape is indicated. The bow is closer to the breech end with little curvature at the muzzle. Again, a fourth-order fit is indicated. The analysis results from SIMBAD indicate very little disturbance at exit because the centroid and 1-sigma dispersion ring is very close to the point of aim. However, the BOOM results indicate otherwise. At the target, BOOM predicts considerable offset of the rounds as well as a 1-sigma ring that is nearly as large as the data. The prediction from BOOM results is much closer to the actual target impacts than that using SIMBAD only.

Results for tube 4106 (DIT tube) are shown in Fig. 4b. The shape of the bore centerline profile is similar to tube 4100, but the magnitudes are different. A third-order fit is appropriate in the vertical plane, whereas a fourth-order fit is appropriate in the horizontal plane. SIMBAD results again indicate very little disturbance at exit, but BOOM results are much closer in location to the actual data. The 1-sigma dispersion ring for both SIMBAD and BOOM are the same as for the previous gun tube, which is 3–5 times less than the actual data.

Results for tube 4994 (STD tube) are shown in Fig. 4c. The shape of the bore centerline profile is significantly different than that of the two earlier DIT tubes. In the vertical plane the bow points upward at the muzzle, and in the horizontal plane very little curvature exists. This is a result of the gravity indexing method in which the preferential plane of bending is indexed to the vertical plane with

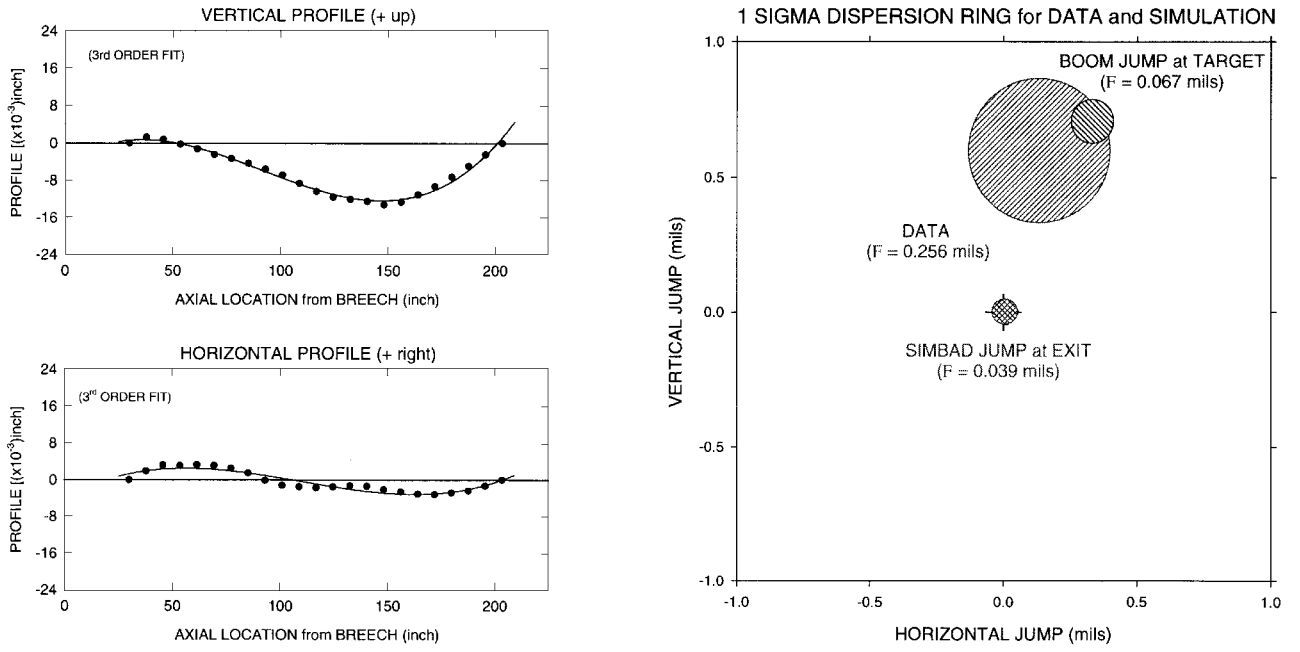

Fig. 4c Comparison of results for tube 4994.

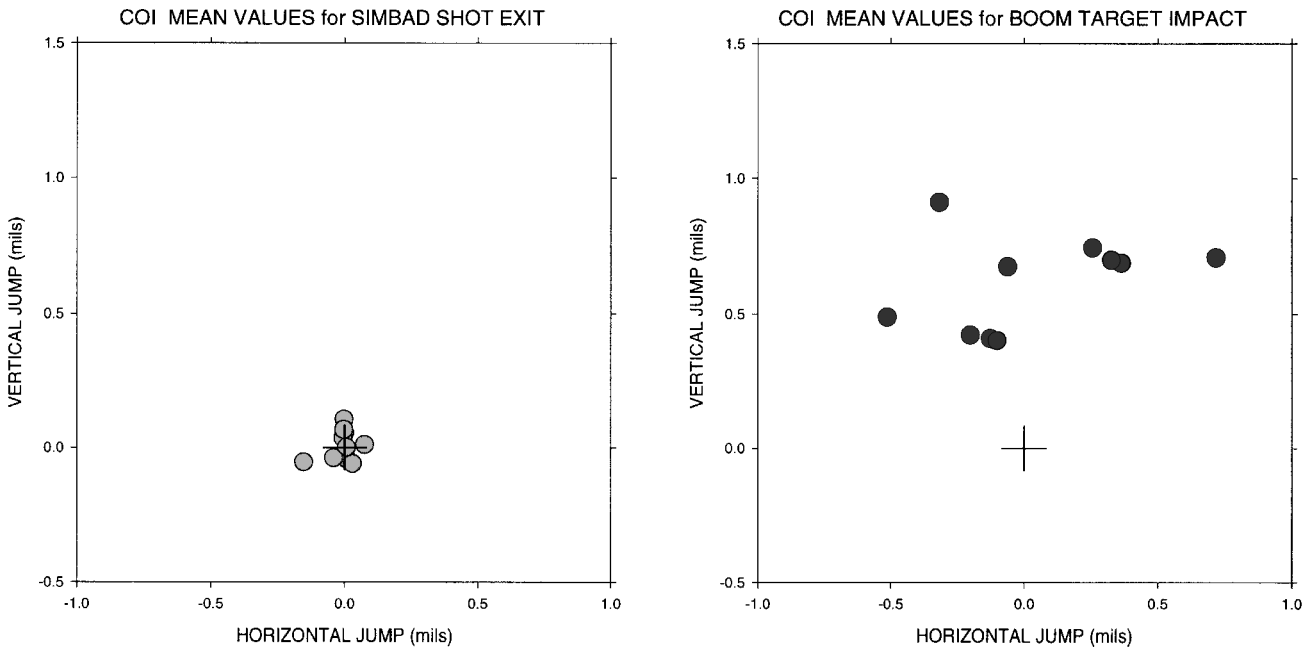

Fig. 5 Comparison of calculated impact mean values results of both models for all tubes.

the muzzle end pointed upward. A third-order fit is appropriate for the data in both planes. SIMBAD results again indicate very little disturbance at exit, but BOOM results are much closer and, in fact, overlap the actual data. The 1-sigma dispersion ring for both SIMBAD and BOOM is of the same order as is that for the previous gun tubes, which, for this tube, is 4–6 times less than the actual data.

A summary of all mean jump values from the analytical results is shown in Fig. 5. The leftmost chart contains the mean jump values generated by the SIMBAD analysis. The rightmost chart contains the mean values of projectile impact point from the BOOM analysis. The impact window is 2.0 × 2.0 mil. The SIMBAD results predict very little perturbation because the mean jump values for all 10 tubes are clustered around the cross hairs. However, the same cannot be said for the BOOM results. The mean values for projectile impact from BOOM analysis are scattered about with none near the aim point. As in Fig. 1, the data values for impact locations are widely scattered. A much better way of comparing the worth of the analytical results is to plot the differential jump mean values on an impact plot. Figure 6 contains this information. A differential jump in the mean is defined as the difference between the mean jump results from firing data and analysis. The leftmost chart contains these values using the SIMBAD analysis, whereas the rightmost chart contains the same using the BOOM analysis. If either model were a perfect predictor, then all differential values would be at the cross hairs. As expected, this is not the case. The differential values from the SIMBAD analysis reside well above and to the right of the cross hairs for nine out of ten tubes. A 1-sigma deviation ring plotted about the axis indicates the dispersion in the differential data. For the SIMBAD results, it is 0.758 mil. On the rightmost chart the differential jump mean values for the BOOM analysis are shown. The deviation ring using this analysis is 0.442 mil. This maps to a 42% improvement in predicting the mean jump values for a series of test shots using the BOOM analysis as compared to the SIMBAD results.

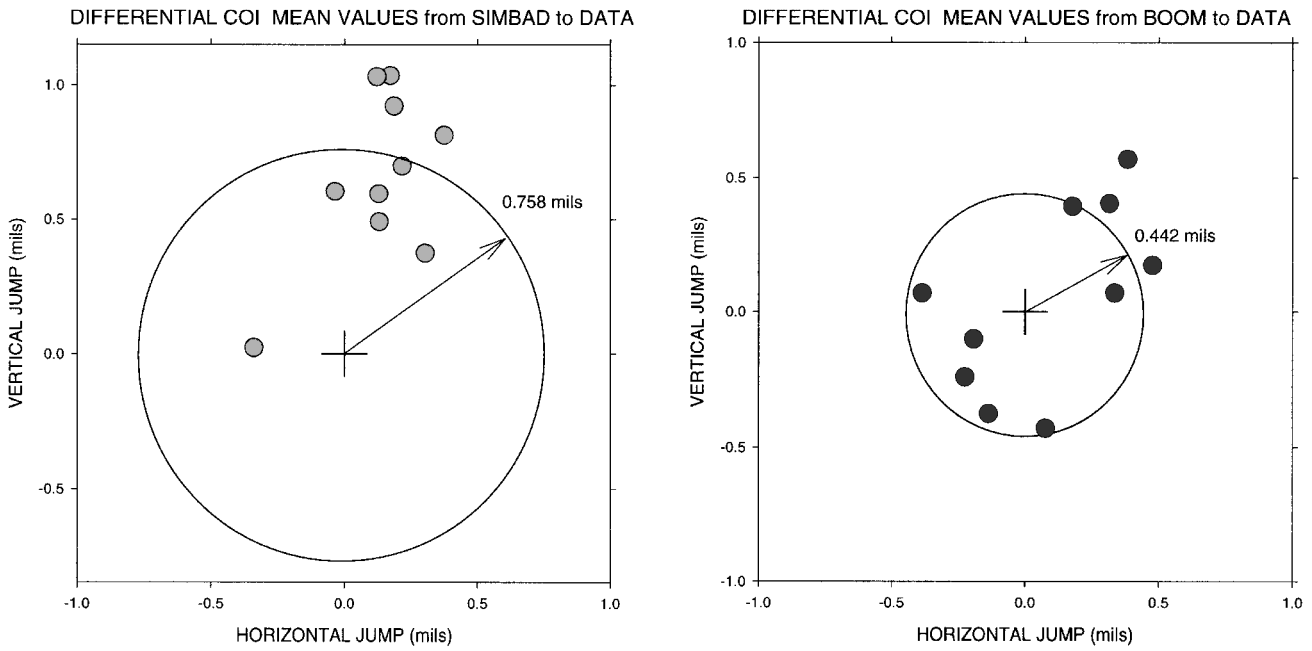

Fig. 6 Comparison of differential results for impact mean values for all tubes.

When the computed results reported herein are compared to the experimental results reported by Bornstein, et al.,[11] the average magnitude of this study's jump values in the vertical plane are about one-half of those reported by Bornstein. In the horizontal plane the results of both are comparable. Additionally, the experimental values in the vertical plane reported for the STD tubes in the DIT test are about two-thirds of those reported by Bornstein. From this it is apparent that impact point dispersion is strongly dependent on field or test conditions and that generalizing results based on one test or analysis should be avoided.

Conclusions

It is impossible to manufacture perfectly straight gun tubes due to their slenderness ratios and propensity to warp during manufacture. Current design specifications restrict the amount of profile deviation between measurement points and along the total length of the tube. The real culprit in regard to dynamic excitation is not profile straightness but rather local curvature. A gun tube may pass profile inspection but it may possess high degrees of curvature along its entire length. A projectile forced to ride along this bumpy path will most certainly cause self-induced vibration and vibration of the tube as well. A better method of specifying bore straightness is to use local and overall curvature. The same type of algorithm used in this analysis to calculate profile and curvature may be incorporated in the inspection loop during tube manufacture. Curvature and profile data should be reported with the acceptance criterion based on both.

Bore profile data for the 10 tubes used in the test was presented along with a method of determining a correct functional fit of the data points using the chi-square statistic. Parameters of this method include both the number of inspection points and the accuracy of the inspection readings. By twice differentiating the profile fitting function, tube curvature is calculated. This tube parameter, which was different for each tube, proved to be critical in the overall analysis. The mean jump values for each gun tube were different, much like those of the data. Results from studying a portion of the data indicate a definite migration of shot impact locations dependent on the indexing method.

The in-bore gun dynamics model is a finite element analysis in which the structure is defined using beam finite elements. The calculation burden using this type of element is small compared to full three-dimensional elements. The degrees of freedom are on the order of hundreds instead of thousands for three-dimensional models. The free-flight projectile model assumes that the projectile is a rigid body possessing only six degrees of freedom, thus minimizing the computational burden of predicting flight trajectories to the target. Although neither model is extremely complex, the coupled version seems to contain enough of the physics of the problem to be quite beneficial in predicting shot impact patterns and dispersions. Computational time per run is relatively low. This is beneficial when simulation is needed in a design environment to rapidly assess critical design parameters and determine sensitivities.

The overall purpose of this analysis was to validate a coupled simulation package for predicting the impact location of test data fired from the M1A1 weapon. The results show good correlation with field-generated test results. We feel that simulation for accuracy from the breech to the target is possible using moderately complex models.

Acknowledgment

Presented at the 9th Annual U.S. Army Gun Dynamics Symposium, 17–19 November, McLean, Virginia.

References

[1]Schmidt, E., "A Method for Indexing Tank Cannon," U.S. Army Ballistic Research Lab., Rept. BRL-IMR-912, Aberdeen Proving Ground, MD, 1988.

[2]Webb, D., Thomas, J., and Carter, R., "M1A1 Tank DIT Experiment: Analysis and Results," U.S. Army Lab. Command, Rept. BRL-MR3962, Aberdeen Proving Ground, MD, 1992.

[3]Gast, R., "Curvature-Induced Motion of 60 mm Guns, Phase 1: Test Results," Benet Labs., Armament Research, Development, and Engineering Center TR ARCCB-TR-92048, Watervliet, NY, 1992.

[4]Gast, R., "Curvature-Induced Motion of 60 mm Guns, Phase 2: Modeling," Benet Labs., Armament Research, Development, and Engineering Center TR ARCCB-TR-94002, Watervliet, NY, 1994.

[5]Etkin, B., *Dynamics of Atmospheric Flight*, Wiley, New York, 1972.

[6]Murphy, C., "Free Flight of Symmetric Missiles," U.S. Army Ballistics Research Lab., Rept. BRL-1216, Aberdeen Proving Ground, MD, 1963.

[7]Von Mises, R., *Theory of Flight*, Dover, New York, 1959.

[8]Costello, M., and Anderson, D., "Effect of Internal Mass Unbalance on the Stability and Terminal Accuracy of a Field Artillery Projectile," AIAA Atmospheric Flight Mechanics Conf., San Diego, CA, 1996.

[9]Borse, G., *Fortran 77 and Numerical Methods for Engineers*, PWS-Kent Publishing, Boston, MA, 1985, pp. 469–471.

[10]Lyon, D., "Radial Stiffness Measurements of 120 mm Tank Projectiles," U.S. Army Research Lab., ARL-TR-392, Aberdeen Proving Ground, MD, 1994.

[11]Bornstein, J., Celmins, I., Plostins, P., and Schmidt, E., "Launch Dynamics of Fin-Stabilized Projectiles," *Journal of Spacecraft and Rockets*, Vol. 29, No. 2, 1992, pp. 171, 172.